

# Biased Metropolis Sampling for Rugged Free Energy Landscapes

Bernd A. Berg<sup>1,2</sup>

<sup>1</sup>*Department of Physics, Florida State University, Tallahassee, FL 32306, USA*

<sup>2</sup>*School of Computational Science and Information Technology  
Florida State University, FL 32306, USA*

**Abstract.** Metropolis simulations of all-atom models of peptides (i.e. small proteins) are considered. Inspired by the funnel picture of Bryngelson and Wolynes, a transformation of the updating probabilities of the dihedral angles is defined, which uses probability densities from a higher temperature to improve the algorithmic performance at a lower temperature. The method is suitable for canonical as well as for generalized ensemble simulations. A simple approximation to the full transformation is tested at room temperature for Met-Enkephalin in vacuum. Integrated autocorrelation times are found to be reduced by factors close to two and a similar improvement due to generalized ensemble methods enters multiplicatively.

## INTRODUCTION

Reliable simulations of biomolecules are one of nowadays grand challenges of computational science. In particular the problem of protein folding thermodynamics starting purely from an amino-acid sequence has received major attention. Until recently the prevailing view has been that it is elusive to search for the native states with present day simulational techniques due to limitations of time scale and force field accuracy. Now a barrier appears to be broken, as it was reported [1] that large scale distributed computing allows to achieve folding of the 23-residue design mini-protein BBA5, which is relatively insensitive to inaccuracies of the force field. The relaxation dynamics of the computer simulation is found to be in good agreement with the experimentally observed folding times and equilibrium constants.

Molecular dynamics (MD) technics, for a review see [2], tend to be the method of first choice for simulations of biomolecules. One of the attractive features of MD is that it allows to follow the physical time evolution of the system under investigation. Nevertheless, there has also been activity based on the Metropolis method [3], which allows only for limited dynamical insights and has its strength in the generation of configurations which are in thermodynamical equilibrium. A major advantage of Metropolis simulations of biomolecules is that they allows for updates which are large moves when one has to follow dynamical trajectories. Such updates may help to overcome the kinetic trapping problem, which is due to a large number of local minima in the free energy space of typical biomolecules. Already Metropolis simulations of the canonical Gibbs-Boltzmann ensemble may jump certain barriers. Using *generalized ensembles*, which enlarge the Gibbs-Boltzmann ensemble and/or replace the canonical weights by other

weighting factors, further progress has been made. For reviews see [4, 5].

To my knowledge *umbrella sampling* [6] was the first generalized ensemble method of the literature. Its potential for applications to a wide range of interesting physical problems remained for a long time dormant. Apparently, one reason was that the computational scientists in various areas shied away from performing simulations with an a-priori unknown weighting factor. As Li and Scheraga put it [7]: “The difficulty of finding such a weighting factor has prevented wide applications of the “umbrella sampling” method to many physical systems.” This changed with the introduction of the multicanonical approach [8] to complex systems [9, 10, 11]. Besides having the luck that the controversy surrounding its first application got quickly resolved by analytical results [12], the multicanonical approach addressed aggressively the problem of finding reliable weights. Nowadays a starter kit of Fortran programs is available on the Web [13].

The replica exchange or parallel tempering (PT) method [14, 15] uses a generalized ensemble which enlarges the canonical configuration space by allowing for the exchange of temperatures within a set of canonical ensembles. In this and other generalized ensembles the Metropolis dynamics at low temperatures can be accelerated by excursions to disordered configurations at higher temperatures. Note that, in contrast to multicanonical simulations, the probabilities of canonically rare configurations are not enhanced by PT. For the purpose of simulating biomolecules PT was, e.g., studied in Ref.[16, 17, 18].

In this article we discuss a biased updating scheme [19], which enhances already the dynamics of canonical Metropolis simulations and is easily integrated into generalized ensemble simulations too. The latter point is illustrated for parallel tempering. The biased updating scheme is inspired by the funnel picture of protein folding [20]. At relatively high temperatures probability densities of the dynamical variables are estimated and used at lower temperatures to enhance the chance of update proposals to lie in the statistically relevant regions of the configuration space. In some sense this is nothing else but an elaboration of the original importance sampling concept of Metropolis et al.[3].

This article is organized as follows. All-atom protein models, the funnel picture and the rugged Metropolis updating are introduced in the next section. In the subsequent section numerical results are presented for the brain peptide Met-Enkephalin. A short summary and conclusions are given in the final section.

## ALL-ATOM PROTEIN MODELS

Proteins are linear polymers of the 20 naturally occurring amino acids. Small proteins are called peptides. The problem of protein folding is to predict (at room temperature and in solvents) the 3d conformations (native structures) from the sequence of amino acids. A conformational energy function models the interactions between the atoms (units kcal/mol):

$$E_{\text{tot}} = E_{\text{es}} + E_{\text{vdW}} + E_{\text{hb}} + E_{\text{tors}} + E_{\text{sol}} . \quad (1)$$

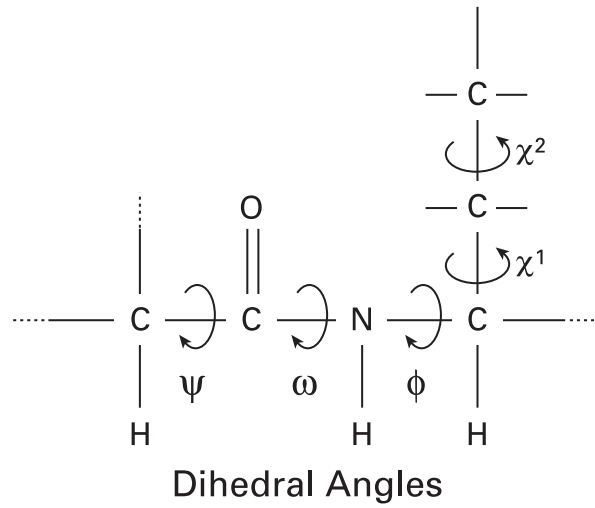


FIGURE 1.

The contributions to the energy function are (charges are in units of the elementary charge):

$$\text{Electrostatic } E_{\text{es}} = \sum_{ij} \frac{332 q_i q_j}{\epsilon r_{ij}}, \quad (2)$$

$$\text{van der Waals } E_{\text{vdW}} = \sum_{ij} \left( \frac{A_{ij}}{r_{ij}^{12}} - \frac{B_{ij}}{r_{ij}^6} \right), \quad (3)$$

$$\text{hydrogen bond } E_{\text{hb}} = \sum_{ij} \left( \frac{C_{ij}}{r_{ij}^{12}} - \frac{D_{ij}}{r_{ij}^{10}} \right), \quad (4)$$

$$\text{torsion } E_{\text{tors}} = \sum_l U_l [1 \pm \cos(n_l \alpha_l)]. \quad (5)$$

The solvent accessible surface method allows for an approximative inclusion of solvent interactions:

$$E_{\text{sol}} = \sum_i \sigma_i A_i, \quad (6)$$

where  $\sigma_i$  is the solvation parameter for atom  $i$  and  $A_i$  the conformation dependent solvent accessible surface area.

The  $r_{ij}$  are the distances between the atoms and the  $\alpha_l$  are the torsion angles for the chemical bonds. The parameters  $q_i, A_{ij}, B_{ij}, C_{ij}, D_{ij}, U_l$  and  $n_l$  are determined from crystal structures of amino acids and a number of thus obtained force fields are given in the literature. Bond length and angles fluctuate little and are normally set constant. The important degrees of freedom are the dihedral angles  $\phi, \psi, \omega$  and  $\chi$ , see Fig.1.

The funnel picture of Bryngelson and Wolynes [20] gives qualitative insight into the process of protein folding, see Fig.2, where a schematic sketch of the free energy versus a suitable *reaction coordinate* is given. However, there is no generical definition of a good reaction coordinate, as the funnel lives in the high-dimensional configuration space. Here

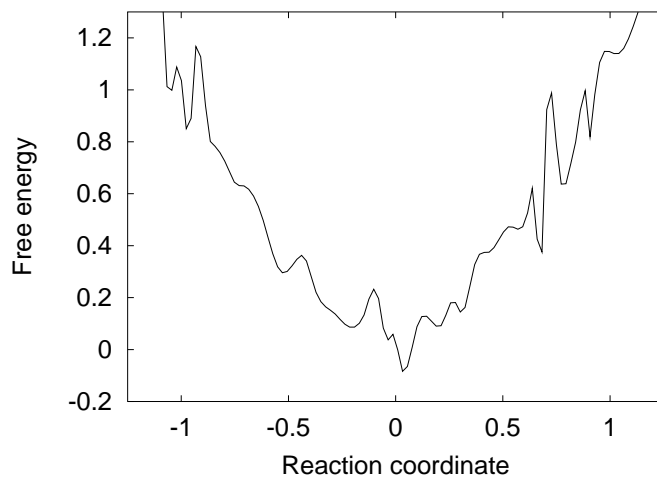


**FIGURE 2.** Funnel picture

we give a parameter free funnel description [19] from higher to lower temperatures, which suggests a method for designing the a-priori Metropolis weights for simulations of biomolecules.

To be definite, we use the all-atom energy function [21] ECEPP/2 (Empirical Conformational Energy Program for Peptides). Our dynamical variables  $v_i$  are then the dihedral angles, each chosen to be in the range  $-\pi \leq v_i < \pi$ , so that the volume of the configuration space is  $K = (2\pi)^n$ . Let us define the *support* of a pd of the dihedral angles. The support of a pd is the region of configuration space where the protein wants to be. Mathematically, we define  $K^p$  to be the smallest sub-volume of the configuration space for which

$$p = \int_{K^p} \prod_{i=1}^n dv_i \rho(v_1, \dots, v_n; T) \quad (7)$$

holds. Here  $0 < p < 1$  is a probability, which ought to be chosen close to one, e.g.,  $p = 0.95$ . The free energy landscape at temperature  $T$  is called *rugged*, if the support of the pd consists of many disconnected parts (this depends of course a bit on the adapted values for  $p$  and “many”). That a protein folds at room temperature, say  $300K$ , into a unique native structure  $v_1^0, \dots, v_n^0$  means that its pd  $\rho(v_1, \dots, v_n; 300K)$  describes small fluctuation around this structure. We are now ready to formulate the funnel picture in terms of pds

$$\rho_r(v_1, \dots, v_n) = \rho(v_1, \dots, v_n; T_r), \quad r = 1, \dots, s, \quad (8)$$

which are ordered by the temperatures  $T_r$ , namely

$$T_1 > T_2 > \dots > T_f. \quad (9)$$

The sequence (8) constitutes a protein *funnel* when, for a reasonable choice of the probability  $p$  and the temperatures (9), the following holds:

1. The pds are rugged.

2. The support of a pd at lower temperature is contained in the support of a pd at higher temperature

$$K_1^p \supset K_2^p \supset \dots \supset K_f^p, \quad (10)$$

e.g. for  $p = 0.95$ ,  $T_1 = 400 K$  and  $T_f = 300 K$ .

3. With decreasing temperatures  $T_r$  the support  $K_r^p$  shrinks towards small fluctuations around the native structure.

Properties 2 and 3 are fulfilled for many systems of statistical physics, when some groundstate stands in for the native structure. The remarkable point is that they may still hold for complex systems with a rugged free energy landscape, i.e., with property 1 added. In such systems one finds typically local free energy minima, which are of negligible statistical importance at low temperatures, while populated at higher temperatures. In simulations at low temperatures the problem of the canonical ensemble approach is that the updating tends to get stuck in those local minima. This prevents convergence towards the native structure on realistic simulation time scales. On the other hand, the simulations move quite freely at higher temperatures, where the native structure is of negligible statistical weight. Nevertheless, the support of a protein pd may already be severely restricted, as we shall illustrate. The idea is to use a relatively easily calculable pd at a higher temperature to improve the performance of the simulation at a lower temperature.

The Metropolis importance sampling would be perfected, if we could propose new configurations  $\{v'_i\}$  with their canonical pd  $\rho(v'_1, \dots, v'_n; T)$ . Due to the funnel property 2 we expect that an *estimate*  $\bar{\rho}(v_1, \dots, v_n; T')$  from some sufficiently close-by higher temperature  $T' > T$  will feed useful information into the simulation at temperature  $T$ . The potential for computational gains is large because of the funnel property 3. The suggested scheme for the Metropolis updating at temperature  $T_r$  is to propose new configurations  $\{v'_i\}$  with the pd  $\bar{\rho}_{r-1}(v'_1, \dots, v'_n)$  and to accept them with the probability

$$P_a = \min \left[ 1, \exp \left( -\frac{E' - E}{kT_r} \right) \frac{\bar{\rho}_{r-1}(v_1, \dots, v_n)}{\bar{\rho}_{r-1}(v'_1, \dots, v'_n)} \right]. \quad (11)$$

This equation biases the a-priori probability of each dihedral angle with an estimate of its pd from a higher temperature. In previous literature [22, 23] such a biased updating has been used for the  $\phi^4$  theory, where it is efficient to propose  $\phi(i)$  at each lattice size  $i$  with its single-site probability.

For our temperatures  $T_r$  the ordering (9) is assumed. With the definition  $\bar{\rho}_0(v_1, \dots, v_n) = (2\pi)^{-n}$  the simulation at the highest temperature,  $T_1$ , is performed with the usual Metropolis algorithm. We have thus a recursive scheme, called rugged Metropolis (RM) in the following. When  $\bar{\rho}_{r-1}(v_1, \dots, v_n)$  is always a useful approximation of  $\rho_r(v_1, \dots, v_n)$ , the scheme zooms in on the native structure, because the pd at  $T_f$  governs its fluctuations.

To get things working, we need to construct an estimator  $\bar{\rho}(v_1, \dots, v_n; T_r)$  from the numerical data of the RM simulation at temperature  $T_r$ . Although this is neither simple nor straightforward, a variety of approaches offer themselves to define and refine the

desired estimators. In the following we work with the approximation

$$\bar{\rho}(v_1, \dots, v_n; T_r) = \prod_{i=1}^n \bar{\rho}_i^1(v_i; T_r) \quad (12)$$

where the  $\bar{\rho}_i^1(v_i; T_r)$  are estimators of reduced one-variable pds defined by

$$\rho_i^1(v_i; T) = \int_{-\pi}^{+\pi} \prod_{j \neq i} dv_j \rho(v_1, \dots, v_n; T) . \quad (13)$$

The implementation of the resulting algorithm, called RM<sub>1</sub>, is straightforward, as estimators of the one-variable reduced pds are easily obtained from the time series of a simulation. The CPU time consumption of RM<sub>1</sub> is practically identical with the one of the conventional Metropolis algorithm.

## NUMERICAL RESULTS

To illustrate the developed ideas, we rely on the brain peptide Met-Enkephalin, which is a numerically well-studied [24, 25, 10, 26, 27]. Met-Enkephalin is determined by the amino-acid sequence Tyr–Gly–Gly–Phe–Met or, in the short notation, Y–G–G–F–M, where

Tyr (Y)	–	Tyrosine
Gly (G)	–	Glycine
Phe (F)	–	Phenylalanine
Met (M)	–	Methionine

Our simulations are performed with a variant of SMMP [28] (Simple Molecular Dynamics for Protein) using fully variable  $\omega$  torsion angles. For the data analysis we keep a times series by writing out configurations every 32 sweeps.

Fig.3 show the probability densities of the dihedral angle  $v_{13}$  (for the notation see Table 1) at 400 K and 300 K. This angle is chosen because it illustrates the possibility of large moves in the Metropolis updating, which jump barriers of a molecular dynamics simulation. Namely, a single update may take us directly from each of the three populated regions to each other, whereas one encounters barriers when one has to move in small increments  $\Delta v_{13}$ .

To evaluate the relative performance of different algorithms, we measure the integrated autocorrelation times  $\tau_{\text{int}}$  for the energy and each dihedral angle. The integrated autocorrelation times are directly proportional to the computer run times needed to achieve the same statistical accuracy. For an observable  $f$  the autocorrelations are

$$C(t) = \langle f_0 f_t \rangle - \langle f \rangle^2 \quad (14)$$

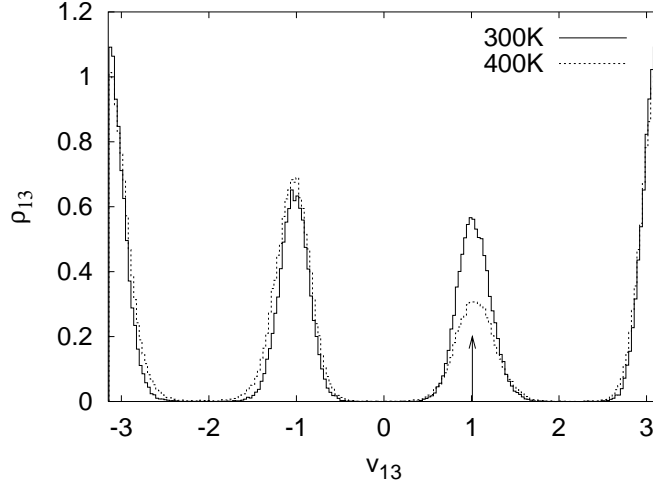


**FIGURE 3.** Probability density of a dihedral angle.

where  $t$  labels the computer time. Defining  $c(t) = C(t)/C(0)$ , the time-dependent integrated autocorrelation time is given by

$$\tau_{\text{int}}(t) = 1 + 2 \sum_{t'=1}^t c(t') . \quad (15)$$

Formally the integrated autocorrelation time  $\tau_{\text{int}}$  is defined by  $\tau_{\text{int}} = \lim_{t \rightarrow \infty} \tau_{\text{int}}(t)$ . Numerically this limit cannot be reached as the noise of the estimator increases faster than the signal. Nevertheless, one can calculate reliable estimates by reaching a window of  $t$  values for which  $\tau_{\text{int}}(t)$  becomes flat, while its error bars are still reasonably small.

Columns 5 and 6 of Table 1 collect our estimates of the integrated autocorrelation times from conventional, canonical Metropolis simulations at 400 K and 300 K. We find a remarkable slowing down. For the energy, which is characteristic for the over-all behavior,  $\tau_{\text{int}}$  increases by a factor of about ten. For certain angles, e.g.  $v_{10}$ ,  $\tau_{\text{int}}$  increases even by factors larger than twenty. At 400 K conventional Metropolis simulations allow to calculate observables with relative ease, while this is no longer the case at 300 K. Our aim is to use information from the 400 K simulation to improve on the performance at 300 K.

One finds that the energy histograms of the 400 K and the 300 K simulation have a considerable overlap, see Fig.4. Therefore, the two temperatures are well-suited to be combined into a PT [14, 15] simulation. We abstain here from introducing additional temperatures, because our aim is to get a clear understanding of the improvement of the 300 K simulation due to PT input from 400 K.

In Fig.5 integrated autocorrelations times for the energy variable are compared at 300 K. The order of the curves agrees with the order in the figure legend. From up to down: Conventional canonical Metropolis simulation, RM<sub>1</sub> improved canonical Metropolis simulation with input from 400 K, PT simulation coupled to 400 K and the RM<sub>1</sub> improved PT simulation. The variable  $t$  of equation (15) is given in units of 32

**TABLE 1.** Integrated autocorrelation times.

$i$	var	res	res	400K	300K	300K	300K	300K
				Metro	Metro	RM <sub>1</sub>	PT	PT+RM <sub>1</sub>
1.	$\chi^1$	Tyr-1	Tyr-1	2.16 (08)	15.8 (2.0)	9.36 (72)	6.28 (46)	3.38 (22)
2.	$\chi^2$	Tyr-1	Tyr-1	1.23 (02)	2.96 (25)	1.68 (08)	1.80 (08)	1.23 (03)
3.	$\chi^6$	Tyr-1	Tyr-1	1.07 (02)	2.00 (12)	1.58 (09)	1.38 (03)	1.10 (02)
4.	$\phi$	Tyr-1	Tyr-1	1.49 (05)	5.77 (48)	3.31 (23)	1.96 (07)	1.91 (13)
5.	$\psi$	Tyr-1	Gly-2	5.02 (14)	62 (13)	30.3 (2.0)	15.9 (1.4)	8.61 (53)
6.	$\omega$	Tyr-1	Gly-2	3.09 (10)	21.1 (1.8)	9.68 (66)	7.85 (36)	4.62 (55)
7.	$\phi$	Gly-2	Gly-2	6.03 (33)	134 (25)	66.6 (7.6)	26.6 (1.6)	13.8 (0.6)
8.	$\psi$	Gly-2	Gly-3	7.49 (50)	185 (37)	91 (13)	30.6 (2.2)	18.2 (1.8)
9.	$\omega$	Gly-2	Gly-3	4.50 (15)	31.4 (2.7)	14.8 (0.9)	14.6 (0.7)	5.51 (31)
10.	$\phi$	Gly-3	Gly-3	7.49 (47)	167 (27)	80.6 (7.0)	32.7 (3.1)	22.6 (2.7)
11.	$\psi$	Gly-3	Phe-4	5.05 (30)	150 (33)	81 (12)	35.9 (3.5)	16.7 (0.8)
12.	$\omega$	Gly-3	Phe-4	3.33 (10)	13.53 (90)	6.71 (56)	7.48 (04)	3.15 (25)
13.	$\chi^1$	Phe-4	Phe-4	1.85 (04)	14.7 (2.7)	5.51 (70)	3.29 (16)	1.71 (06)
14.	$\chi^2$	Phe-4	Phe-4	1.18 (03)	1.77 (08)	1.42 (07)	1.19 (04)	1.10 (02)
15.	$\phi$	Phe-4	Phe-4	6.60 (19)	116 (24)	57.9 (4.2)	30.9 (2.7)	15.7 (1.2)
16.	$\psi$	Phe-4	Met-5	9.17 (56)	191 (35)	88 (12)	40.3 (3.2)	20.8 (1.5)
17.	$\omega$	Phe-4	Met-5	1.96 (07)	7.71 (90)	4.57 (41)	3.46 (22)	1.91 (11)
18.	$\chi^1$	Met-5	Met-5	1.61 (07)	10.8 (1.5)	7.59 (85)	4.50 (41)	3.51 (24)
19.	$\chi^2$	Met-5	Met-5	1.19 (02)	1.68 (05)	1.16 (03)	1.30 (04)	1.12 (04)
20.	$\chi^3$	Met-5	Met-5	1.01 (01)	1.05 (02)	1.04 (02)	1.04 (02)	1.01 (01)
21.	$\chi^4$	Met-5	Met-5	1.00 (01)	1.01 (01)	1.00 (01)	1.01 (01)	1.01 (01)
22.	$\phi$	Met-5	Met-5	2.77 (10)	31.4 (2.9)	20.8 (1.9)	14.9 (1.1)	9.16 (76)
23.	$\phi$	Met-5	Met-5	1.54 (05)	21.4 (2.3)	13.9 (1.7)	7.83 (48)	3.73 (19)
24.	$\omega$	Met-5	Met-5	1.06 (01)	1.14 (02)	1.03 (02)	1.08 (01)	1.03 (02)
	$E$			4.98 (20)	49.6 (5.0)	26.2 (1.6)	19.9 (1.6)	9.94 (60)

sweeps due to the way our data are recorded. In the range shown, i.e. up to  $t = 200 \times 32$  sweeps, a window exist for the PT and the RM<sub>1</sub> improved PT simulations, which allows to estimate the integrated autocorrelation times of these simulations. For the other two simulations one has to go to even larger  $t$  values, but it remain possible to estimate  $\tau_{\text{int}}$ . For the energy and all 24 dihedral angles the  $\tau_{\text{int}}$  estimates are collected in Table 1.

For the energy we find a decrease from  $\tau_{\text{int}} \approx 50$  to  $\tau_{\text{int}} \approx 25$  due to the RM<sub>1</sub> improvement of the canonical Metropolis simulation, i.e. approximately a factor of 2. The PT improvement of this simulation is even larger, namely from  $\tau_{\text{int}} \approx 50$  to  $\tau_{\text{int}} \approx 20$ , i.e. approximately a factor of 2.5. In both cases the CPU time spent at 400K is not part of the equation. This is justified as one should anyway understand the



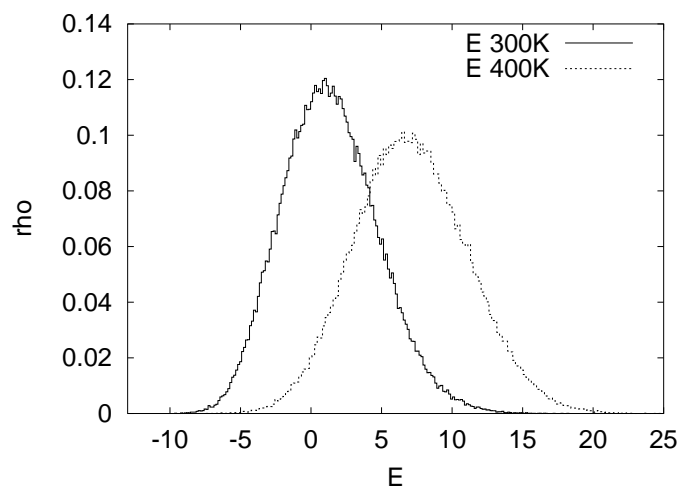


**FIGURE 4.** Met-Enkephalin (internal) energy histograms at 300 K and 400 K.

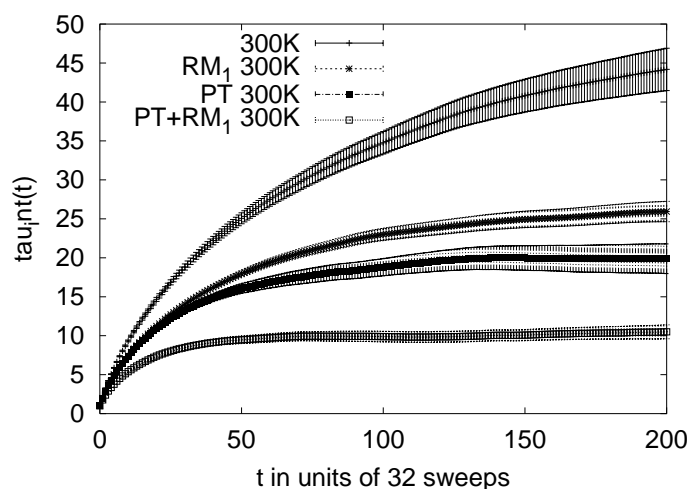


**FIGURE 5.** Integrated autocorrelation times for the energy at 300 K.

system first at temperatures where one does not suffer from long autocorrelation times. For PT the factor 2.5 is the improvement in real time when two identical PC nodes with some parallel software like MPI (Message Passing Interface) are available. Most remarkably, the two improvements multiply: For the  $RM_1$  improved PT simulation the autocorrelation time is down to  $\tau_{\text{int}} \approx 10$ , only about one more factor of two away from the  $\tau_{\text{int}}$  value at 400 K.

Inspection of the  $\tau_{\text{int}}$  values for the 24 dihedral angles shows large differences. For the conventional canonical simulation the range is from<sup>1</sup>  $\tau_{\text{int}} \approx 1$  for  $v_{21}$  to  $\tau_{\text{int}} \approx 200$  for

<sup>1</sup> A value  $\tau_{\text{int}} = 1$  means that our resolution of measurements every 32 sweeps is too crude to show the autocorrelations, which one may still expect on the scale of a few sweeps.

$v_{16}$ . For the PT-RM<sub>1</sub> simulation it becomes reduced to a range from  $\tau_{\text{int}} \approx 1$  to  $\tau_{\text{int}} \approx 20$ . This suggests that it is not efficient to simulate by sweeps, where each dihedral angle is updated once per sweep. Instead, an algorithm (systematic or random) where the number of updates per angle is proportional to its integrated autocorrelation time is expected to be more efficient. Obviously, this can be implemented without major changes of the existing code, but tests of this idea have not yet been completed. After all these improvements the 300 K simulation is expected to be no more autocorrelated than the conventional, canonical simulation at 400 K.

All-atom Metropolis simulations of small biomolecules deserve a place on their own in the arsenal of computational biophysics. A good understanding of smaller pieces of a larger protein is one of the ingredients, which can pave the way towards the understanding of large systems like proteins. Major algorithmic problems remain to be solved before Metropolis simulations of all-atom models may become directly suitable for applications like the folding of small to medium sized proteins.

One algorithmic problem is that of correlated moves of two or more dihedral angles. Such moves promise to overcome (jump) essential free energy barriers in the case of larger molecules. Within conventional canonical Metropolis simulations the acceptance rates for simultaneous moves of two and more angles are prohibitively small. The RM concept promises major inroads, but details have not yet been tested out.

An even more challenging problem is the inclusion of solvent effects. Here the large moves of Metropolis updates create the *cavity problem*. We need a cavity in the surrounding water to accommodate the move and updates of the dihedral angles do not create one. This appears to be one of the major reasons why large scale simulations of proteins with a surrounding solvent are to an overwhelming extent done within the MD framework, where the cavity problem is avoided due to joint, small moves of all degrees of freedoms. Within the Metropolis approach effective solvent models may provide a solution. They are, e.g., defined by a solvent contribution like  $E_{\text{sol}}$  in Eq.(6). Unfortunately, no reliable determination of the parameters entering this equation exists presently in the literature, as was demonstrated by recent simulations [29, 30]. However, it appears to be within the reach of Metropolis simulations to lead the way towards determining reliable parameterizations.

## SUMMARY AND CONCLUSIONS

- The RM<sub>1</sub> approximation to the rugged Metropolis (RM) method [19] leads already to considerable improvements over conventional Metropolis simulations of Met-Enkephalin at 300K. As RM<sub>1</sub> is easily implemented and needs no additional computer time, it should be used whenever Metropolis simulations of suitable systems are done.
- For larger systems one-variable moves alone will not work due to correlations between the dihedral angles. The RM approach promises sufficiently large acceptance rates for multi-variable moves.
- Ultimately, each biomolecule of interest may need its own, specifically designed, Metropolis algorithm. This task includes to determine reliable parameters for a

solvent model like the one of Eq.(6).

## ACKNOWLEDGMENTS

I am indebted to Yuko Okamoto for many useful discussion and to Robert Swendsen for kindly informing me during this meeting about a dynamically optimized Monte Carlo method [31], which is tailored for the simulation of biomolecules. Further, I would like to thank James Gubernatis and the other organizers of the Los Alamos Metropolis workshop for their kind hospitality. This work was partially supported by the U.S. Department of Energy under contract No. DE-FG02-97ER41022.

## REFERENCES

1. Snow, C.D., Nguyen, H., Pande, V.S., and Gruebele, M., *Nature*, **420**, 102–106 (2002).
2. Frenkel, D., and Smit, B., *Understanding Molecular Simulation*, Academic Press, San Diego, 1996.
3. Metropolis, N., Rosenbluth, A.W., Rosenbluth, M.N., Teller, A.H., and Teller, E., *J. Chem. Phys.*, **21**, 1087–1092 (1953).
4. Mitsutake, A., Sugita, Y., and Okamoto, Y., *Biopolymers (Peptide Science)*, **60**, 96–123 (2001).
5. Berg, B., *Comp. Phys. Commun.*, **104**, 52–57 (2002).
6. Torrie, G.M., and Valleau, J.P., *J. Comp. Phys.*, **23**, 187–199 (1977).
7. Li, Z., and Scheraga, H.A., *J. Mol. Struct. (Theochem)*, **179**, 333–352 (1988).
8. Berg, B.A., and Neuhaus, T., *Phys. Rev. Lett.*, **68**, 9–12 (1992).
9. Berg, B.A., and Celik, T., *Phys. Rev. Lett.*, **69**, 2292–2295 (1992).
10. Hansmann, U.H., and Okamoto, Y., *J. Comp. Chem.*, **14**, 1333–2338 (1993).
11. Hao, M.H., and Scheraga, H.A., *J. Phys. Chem.*, **98**, 4940–4948 (1994).
12. Borgs, C., and Janke, W., *J. Phys. I France* **2**, 2011–2018 (1992).
13. Berg, B.A., *cond-mat/0206333*, to appear in *Comp. Phys. Commun.* .
14. Geyer, G.J., in *Proceedings of the 23rd Symposium of the Interface*, Interface Foundation, Fairfax, Virginia (1991).
15. Hukushima, A., and Nemoto, K., *J. Phys. Soc. Jpn.*, **65**, 1604–1608 (1996).
16. Hansmann, U.H., *Chem. Phys. Lett.*, **281**, 140–150 (1997).
17. Sugita, Y., and Okamoto, Y., *Chem. Phys. Lett.*, **314**, 141–151 (1999).
18. Rhee, Y.M., and Pande, V.S., *Biophys. J.*, **84**, 775–786 (2003).
19. Berg, B.A., *Phys. Rev. Lett.*, **90**, 180601 (2003).
20. Bryngelson, D., and Wolyness, P.G., *Proc. Nat. Acad. Sci. USA*, **84**, 7524–7528 (1987).
21. M.J. Sippl, M.j., Nemethy, G., and Scheraga, H.A., *J. Phys. Chem.*, **85**, 6611–6233 (1984).
22. Bruce, A.D., *J. Phys. A*, **14**, L749–L784 (1985).
23. Milchev, A., Heermann, D.W., and Binder, K., *J. Stat. Phys.*, **44**, 749–784 (1986).
24. Li, Z., and Scheraga, H.A., *Proc. Nat. Acad. Sci. USA*, **85**, 6611 (1987).
25. Okamoto, Y., Kikuchi, T., and Kawai, H., *Chem. Lett.*, **1992**, 1275–1278 (1992).
26. Meirovitch, H., Meirovitch, E., Michel, A.G., and Vásquez, M., *J. Phys. Chem.*, **98**, 6241–6243 (1994).
27. Hansmann, U.H., Okamoto, Y., and Onuchic, J.N., *PROTEINS*, **34**, 472–483 (1999).
28. Eisenmenger, F., Hansmann, U.H., Hayryan, S., and Hu, C.-K., *Comp. Phys. Commun.*, **138**, 192–212 (2001).
29. Peng, Y., and Hansmann, U.H., *Biophys. J.*, **82**, 3269–3276 (2003).
30. Berg, B.A., and Hsu, H.-P., *cond-mat/0306435*.
31. Bouzida, D., Kumar, S., and Swendsen, R., *Phys. Rev. A*, **45**, 8894–8901 (1992); *Proceedings of the Twenty-Sixth Annual Hawaii International Conference on System Sciences*, Ed. Mudge, T.N., Milutinovic, V., and Hunter, L. (IEEE Computer Society Press), pp.736–742 (1993).